ECRONICON OPEN ACCESS

EC DENTAL SCIENCE
Research Article

Advancing Biomaterials with Lithium and Strontium Modified Bioactive Glass: Characterization and Standardization

Labanya Biswas*, Abhijit Chakraborty, Biswanath Kundu and Parijat Chakraborty

Department of Periodontology, Guru Nanak Institute of Dental Sciences and Research, Kolkata, West Bengal, India

***Corresponding Author:** Labanya Biswas, Department of Periodontology, Guru Nanak Institute of Dental Sciences and Research, Kolkata, West Bengal, India.

Received: May 13, 2024; **Published:** June 07, 2024

DOI: 10.31080/ECDE.2024.23.02146

Abstract

A bioactive glass compound is able to bind to bone tissue and promote new bone growth with osteostimulating effects. Various ions, like copper (Cu), zinc (Zn), silver (Ag) and manganese (Mn) have been used previously to enhance pro-osteogenic property. We aim to regenerate the lost alveolar bone with the properties of bioglass along with adding the best properties of lithium and strontium ions as well. The conventional glass melting method was used in the production of bioactive glass. *In vitro* characterization of the material was done using parameters like XRD, FTIR and AP-BD.

Keywords: *Regeneration; Periodontium; Bioactive Glass; Lithium; Strontium*

Introduction

Periodontal therapy helps to slowdown or stop the progression of destruction in periodontal tissue in order to improve its long-term prognosis. The World Workshop on Periodontics (1996) discussed three methods for regenerating lost periodontal bone i.e. defect debridement, bone grafting, and tissue regeneration [1]. A perfect graft material would stimulate osteogenesis and cementogenesis, leading to the formation of a new periodontal attachment complex. In 1969, Hench., *et al*. first developed bioactive glass [2] which represents a bunch of reactive materials capable of binding to mineralized tissue. A bioactive glass compound is able to bind to bone tissue and promote new bone growth with osteostimulating effects [3]. Various ions, like copper (Cu), zinc (Zn), silver (Ag) and manganese (Mn) have been used previously to enhance pro-osteogenic property [4]. These methods involve the incorporation of different metal ions into the silicate network, aiming to improve the overall performance of doped bioactive glass materials and positively enhance bone formation [5]. Lithium doped bioactive glasses (55% SiO_2, 36% CaO, 4% P_2O_5, 5% Li_2O) synthesized by a rapid alkaline salt-gel method which stimulates the formation of apatite [5]. Lao., *et al*. found in a *vitro* study that bioactivity of Sr-doped bioactive glasses is higher than conventional bioactive glass [6].

Keeping in mind the above we aim to regenerate the lost alveolar bone with the properties of Bioglass along with adding the best properties of lithium and strontium ions as well. For which we firstly aim to characterise the multi-ion doped bioactive glass and check its efficacy in hard and soft tissue regeneration.

Materials and Methodology

Bioactive glass powder preparation: The conventional glass melting method was used in the production of bioactive glass. Appropriate amounts of reagents (Table 1) were taken and mixed homogeneously using the mixer. Then the mixture was melted in a platinum crucible at 1450°C inside the furnace.

Reagent	BAG	Li-BAG	Sr-BAG	Li-Sr-BAG
SiO_2	57.33%	57.33%	57.33%	57.33%
Na_2O	10.41%	10.16%	10.41%	10.16%
CaO	21.64%	21.64%	20.64%	20.64%
P_2O_5	5.96%	5.96%	5.96%	5.96%
TiO_2	1.29%	1.29%	1.29%	1.29%
B_2O_3	3.37%	3.37%	3.37%	3.37%
LiO_2		0.25%		0.25%
SrO_2			1%	1%

Table 1: *Final composition of sample groups.*

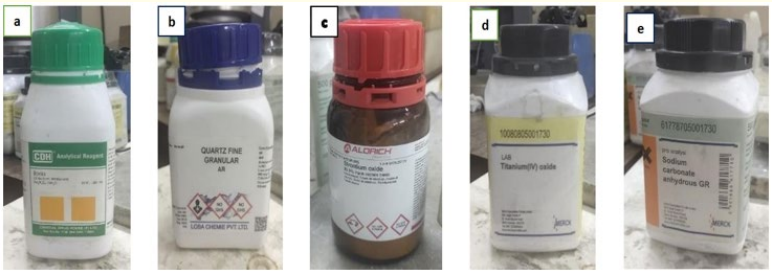

Figure 1: *Reagents: a. Anhydrous borax; b. Silica; c. Strontium oxide; d. Titanium oxide and e. Sodium carbonate.*

Homogeneity was maintained during melting using glass rod, after melting the liquid glass material was quenched in a pot filled with distil water and frit of glass is obtained. Then the frit was dried in the drier at 80°C. The frit of glasses were grinded manually in a stainless-steel mortar-pestle and then sieved in 50 mess sieve and milled for six hours in a low-energy ball mill with acetone, again it was dried in drier at 80°C.

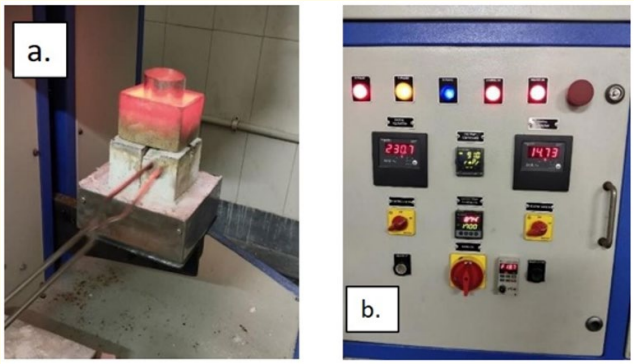

Figure 2: *a. Melting at 1450°C in furnace and b. Furnace programming.*

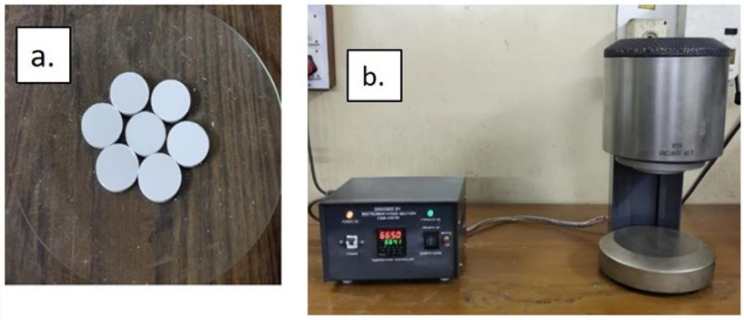

Figure 3: *a. Pallets formed using the mould and b. Sintering at 650°C in dental furnace.*

Scaffold preparation: The milled glass was first crushed to obtain the powder. Then the glass powder mixed with an equal amount (ratio of 50:50 wt%) of naphthalene (< 30µ) which is a porogen. Then pallet was formed from this mixture using mould. The pallets were compacted in a 150 MPa cold isostatic press followed by sintering at 675°C except for LS-BAG (650°C) on a platinum-plate for 6 minutes. Then the scaffolds were crushed and sterilized by gamma radiation. The samples were finally stored in a vacuum desiccator until further use.

In vitro characterization of bioactive glass powders

- **X-ray diffraction (XRD):** XRD is an analytical technique for determining phase composition, crystal structure, and orientation of powder, solid, and liquid samples.
- **FTIR spectroscopy:** A method for getting an infrared spectrum of absorption or emission from a solid, liquid, or gas can be Fourier-transform infrared spectroscopy.
- **AP BD:** We assessed the apparent porosity (AP) to find out how many pores were in our prepared samples.

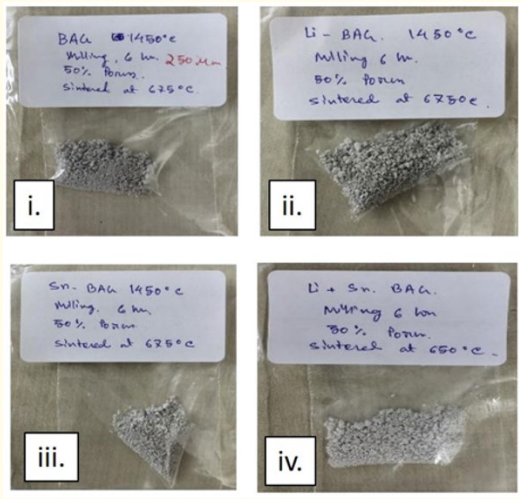

Figure 4: *Samples i-iv after gamma ray sterilization.*

Results and Observation

XRD: Using XRD at a diffraction angle of 10-80°2θ, the phase of the produced powders was examined.

Key points:

- The XRD patterns confirm the amorphous nature of the material after heat treatment for all compositions studied.
- This is indicated by the broad diffraction peak observed between 20° and 35° 2θ, which signifies structural disorder and a glassy structure.
- Adding dopants resulted in very minor changes to the amorphous characteristics and did not lead to the formation of any crystalline peaks.
- Overall, the glassy structure of the base material remained largely unaffected by the dopant addition.

FTIR: In the FTIR analysis process, test materials are scanned with infrared light to observe their chemical characteristics to confirm the existence of functional groups.

Key points:

- Hydroxyl (-OH): The presence of a band around 3445 cm^{-1} indicates the presence of hydroxyl groups. The broadness of the band suggests intermolecular hydrogen bonding.
- Silicates: The bands at 465 cm^{-1} and 1020 cm^{-1} correspond to Si-O-Si stretching and bending vibrations, respectively. This confirms the presence of silicate groups in the powders.
- Silanols (Si-OH): The bands between 780 - 980 cm^{-1} are attributed to the symmetric stretch of Si-OH groups. This further supports the presence of hydroxyl groups bonded to silicon atoms.

AP & BD: The porous scaffolds were initially physically characterized using the aqueous displacement method (Archimedes' principle) in terms of bulk density (B.D.) and open or apparent porosity (A.P.).

Pore size:

1. BAG and Li-BAG: Average pore size is around 20 μm, with micro- and macro-pores present. Li-BAG also has small pores (1 - 2 μm) throughout its structure.
2. Sr-BAG: Average pore size is 47 μm, with a bi-modal distribution of micro- and macro-pores.
3. Li-Sr-BAG: Average pore size is 8 μm, mainly micro- pores with some small pores (1 - 2 μm).

Porosity and density:

1. BAG and Sr-BAG have similar apparent porosity and higher bulk density compared to Li-BAG and Li-Sr- BAG due to their larger average pore size.
2. Li-BAG and Li-Sr-BAG have higher open porosity and lower bulk density due to their smaller average pore size and presence of additional small pores.

Key points:

- Li-containing materials (Li-BAG and Li-Sr-BAG) had more amorphous content compared to Sr-BAG and BAG.
- Li likely caused "solute-drag" effect during solidification, leading to increased open porosity and lower bulk density in Li-containing samples.

- Sr did not seem to significantly impact the porosity-density relationship like Li did.
- Porosity of Sr-containing (Sr-BAG and Li-Sr-BAG) and BAG were more closely related to the amount of naphthalene added in the preparation stage.

Discussion

Regenerative therapy is mostly limited to certain types of periodontal abnormalities. Research is looking for strategies to increase predictability and extend indications. Indications of periodontal regeneration therapy are- deep intrabony pocket, furcation defect and gingival recession [7,8]. Marc L Nevins., *et al*, Ji Sook Park., *et al*. and many more authors had performed their study on periodontal regeneration in intrabony defect cases. So, we also chose deep intrabony defect aiming regeneration in it [9,10].

Periodontal regeneration therapy includes placement of bone graft, GTR membrane or combination of both. At the moment, the widespread usage of combinations of existing medicines can occasionally improve clinical outcomes. Sculean., *et al*. 2008 observed periodontal tissue regeneration with the use of barrier membranes and graft [11]. We, here in our study bone graft along with GTR membrane is used as regeneration therapy.

The current study was performed to overview on characterisation and determination of efficacy of doped bioactive glass as regenerative material. Characterization is done using XRD, FTIR and AP, BD and efficacy is evaluated by measuring pocket probing depth, relative attachment loss and bone height. Decreasing probing depth, attachment loss and bone loss may help us to understand the new attachment or bone regrowth which influences the soft tissue and hard tissue regeneration.

The functional groups and chemical structure of synthesized materials were analyzed using an Equinox [12] FTIR spectrometer at 400 - 4000 cm^{-1} (100 scans). FTIR spectroscopy was carried out by combining the test material with potassium bromide (KBr) and generating pill disks. The “wavenumber” is shown on the X-axis of the FTIR spectrum, while the absorption values are represented on the vertical axis as “percent transmittance” (T%).

In our study, the FTIR spectra of the identical powders demonstrate:

- Hydroxyl (-OH): The presence of a band around 3445 cm^{-1} indicates the presence of hydroxyl groups. The broadness of the band suggests intermolecular hydrogen bonding.
- Silicates (Si-O-Si): The bands at 465 cm^{-1} and 1020 cm^{-1} correspond to Si-O-Si stretching and bending vibrations, respectively. This confirms the presence of silicate groups in the powders.
- Silanols (Si-OH): The bands between 780-980 cm^{-1} are attributed to the symmetric stretch of Si-OH groups. This further supports the presence of hydroxyl groups bonded to silicon atoms.

According to Chengtie Wu., *et al*. [13] FTIR examination revealed additional P-O peaks showed at wavenumbers of 568, 601, and 1035 cm^{-1} for all Sr-MBG scaffolds, confirming the production of apatite on the surface of Sr-MBG scaffolds.

Khorami., *et al*’s 2011 paper on the FTIR spectra of glasses revealed that [14]:

- Si-O-Si group: FTIR spectra of various glasses exhibit characteristic bands at 470, 790, 1090, and 1250 cm^{-1}, corresponding to bending, symmetric stretching, asymmetric stretching and bending modes of the Si-O-Si group, respectively.
- Si-O group: An additional band at 950 cm^{-1} indicates the presence of Si-O groups with one non-bridging oxygen atom.
- P-O Groups: In Li(3) and Li(7) spectra, a single band at 570 cm^{-1} suggests the presence of amorphous P-O stretching vibrations.

- Apatite: In Li(0) and Li(12) spectra, two resolved peaks at 570 and 600 cm^{-1} indicate crystalline apatite, along with overlapping P-O stretching at 1050 cm^{-1}.
- Carbonate groups: Carbonate groups replacing phosphate groups in the apatite lattice manifest as C-O stretching bands at 870 and 1422 cm^{-1}.
- Carbonate phase: Li(0) and Li(12) exhibit two resolved C-O bands (1422 and 1482 cm^{-1}), suggesting a larger amount of carbonated apatite on their surfaces.

Using FTIR M Fahti., *et al*. observed a well-defined phosphate signal (P-O stretching peak) was seen around 1000 - 1200 cm^{-1}, indicating an amorphous CaO-P_2O_5 rich layer. In addition, FTIR spectra revealed a P-O bending peak at 550 - 620 cm^{-1}.

The characteristics of different types of BAG materials, focusing on their pore size and porosity. Here's a breakdown of key points.

Pore size:

- BAG and Li-BAG: 20 µm average, with small pores (1 - 2 µm) throughout. Li-BAG also has larger pores ranging from 20 - 230 µm.
- Sr-BAG: 47 µm average, with bi-modal distribution of small (1 - 2 µm) and larger (10 - 20 µm) pores.
- Li-Sr-BAG: 8 µm average, with small (1 - 2 µm) pores and larger pores ranging from 10 - 50 µm.

Porosity:

- BAG and Sr-BAG: Similar percentage of apparent porosity to the naphthalene content used in their preparation.
- Li-BAG and Li-Sr-BAG: Significantly higher percentage of open porosity compared to BAG and Sr-BAG.

Density:

- BAG and Sr-BAG: Higher bulk density due to lower open porosity.
- Li-BAG and Li-Sr-BAG: Lower bulk density due to higher open porosity.

Explanation:

- Lithium (Li) promotes coarsening: The presence of Li coarsens the particles, resulting in larger pores and higher open porosity in Li-BAG and Li-Sr-BAG compared to BAG and Sr-BAG.
- Strontium (Sr) has less impact: Sr does not have the same coarsening effect as Li.

Conclusion

Innovative research on bone tissue engineering has made considerable strides over the few decades in the development of new materials, processing techniques and their evaluation and applications. In summary, this study doped Sr and Li ions in bioactive glass in the lab. All bioactive glass samples both doped and undoped were standardized and characterized using methods like XRD and FTIR. Metallic ion doping with the presently available bioactive glass improves the biological performance of the material that may open a new vista in bone tissue engineering. Future research by using these samples *in vivo* will help us compare their benefits or advantages over undoped bioactive glasses in bone healing as well as coating of several metallic implants.

Bibliography

1. Nyman S., *et al*. "New attachment following surgical treatment of human periodontal disease". *Journal of Clinical Periodontology* 9.4 (1982): 290-296.

2. Hench LL., *et al*. "Bonding mechanisms at the interface of ceramic prosthetic materials". *Journal of Biomedical Materials Research* 5.6 (1971): 117-141.

3. Karasu B., *et al*. "Bioactive glasses". *El-Cezerî Journal of Science and Engineering* 4.3 (2017): 436-471.

4. Skallevold HE., *et al*. "Bioactive glass applications in dentistry". *International Journal of Molecular Sciences* 20.23 (2019): 5960.

5. Khan PK., *et al*. "Influence of single and binary doping of strontium and lithium on *in vivo* biological properties of bioactive glass scaffolds". *Scientific Reports* 6.1 (2016): 32964.

6. Workie AB and Sefene EM. "Ion-doped mesoporous bioactive glass: preparation, characterization, and applications using the spray pyrolysis method". *RSC Advances* 12.3 (2022): 1592-1603.

7. Silva AV., *et al*. "Influence of strontium on the biological behavior of bioactive glasses for bone regeneration". *Materials* 16.24 (2023): 7654.

8. Tanushree Rastogi. "Recent advances in periodontal regeneration". Notion Press 1st edition.

9. Nevins ML., *et al*. "Evaluation of periodontal regeneration following grafting intrabony defects with bio-oss collagen: a human histologic report". *International Journal of Periodontics and Restorative Dentistry* 23.1 (2003): 9-17.

10. Lindhe J., *et al*. "Lindhe's clinical periodontology and implant dentistry". Wiley-Blackwell (2021).

11. Sculean A., *et al*. "Regeneration of periodontal tissues: combinations of barrier membranes and grafting materials-biological foundation and preclinical evidence. A systematic review". *Journal of Clinical Periodontology* 35.8 (2008): 106-116.

12. Miguez-Pacheco V., *et al*. "Development and characterization of lithium-releasing silicate bioactive glasses and their scaffolds for bone repair". *Journal of Non-Crystalline Solids* 432 (2016): 65-72.

13. Wu C and Chang J. "Strontium-containing mesoporous bioactive glass for regeneration of osteoporotic bone and periodontal tissue". In Nanobioceramics for Healthcare Applications (2017): 187-212.

14. Khorami M., *et al*. "*In vitro* bioactivity and biocompatibility of lithium substituted 45S5 bioglass". *Materials Science and Engineering: C* 31.7 (2011): 1584-1592.

15. Zhang Q., *et al*. "Lithium-calcium-silicate bioceramics stimulating cementogenic/osteogenic differentiation of periodontal ligament cells and periodontal regeneration". *Applied Materials Today* 16 (2019): 375-387.

16. Balamurugan A., *et al*. "Synthesis and characterisation of sol gel derived bioactive glass for biomedical applications". *Materials Letters* 60.29-30 (2006): 3752-3757.

17. Kaur G., *et al*. "A review of bioactive glasses: their structure, properties, fabrication and apatite formation". *Journal of Biomedical Materials Research Part A: An Official Journal of The Society for Biomaterials, The Japanese Society for Biomaterials, and The Australian Society for Biomaterials and the Korean Society for Biomaterials* 102.1 (2014): 254-274.

18. Cannillo V., *et al*. "Bioactive glasses in periodontal regeneration: existing strategies and future prospects-a literature review". *Materials* 15.6 (2022): 2194.

19. Abushahba F., *et al*. "Bioactive glasses in periodontal regeneration: a systematic review". *Tissue Engineering Part C: Methods* 29.5 (2023): 183-196.

20. Park JS., *et al*. "Effects of pretreatment clinical parameters on bioactive glass implantation in intrabony periodontal defects". *Journal of Periodontology* 72.6 (2001): 730-740.

21. Koo KT., *et al*. "Periodontal repair in dogs: guided tissue regeneration enhances bone formation in sites implanted with a coral-derived calcium carbonate biomaterial". *Journal of Clinical Periodontology* 32.1 (2005): 104-110.

22. Melcher AH. "On the repair potential of periodontal tissues". *Journal of Periodontology* 47.5 (1976): 256-260.

Volume 23 Issue 7 July 2024